

CellMixer: Annotation-free Semantic Cell Segmentation of Heterogeneous Cell Populations

**Mehdi Naouar^{1,2,*}, Gabriel Kalweit^{1,2}, Anusha Klett^{2,3}, Yannick Vogt^{1,2},
 Paula Silvestrini², Diana Laura Infante Ramirez^{2,3,5}, Roland Mertelsmann^{2,3},
 Joschka Boedecker^{1,2,4}, Maria Kalweit^{1,2}**

¹University of Freiburg, ²Collaborative Research Institute Intelligent Oncology (CRIION)

³University Medical Center Freiburg, ⁴BrainLinks-BrainTools, ⁵University of Buenos Aires

Abstract

In recent years, several unsupervised cell segmentation methods have been presented, trying to omit the requirement of laborious pixel-level annotations for the training of a cell segmentation model. Most if not all of these methods handle the instance segmentation task by focusing on the detection of different cell instances ignoring their type. While such models prove adequate for certain tasks, like cell counting, other applications require the identification of each cell’s type. In this paper, we present CellMixer, an innovative annotation-free approach for the semantic segmentation of heterogeneous cell populations. Our augmentation-based method enables the training of a segmentation model from image-level labels of homogeneous cell populations. Our results show that CellMixer can achieve competitive segmentation performance across multiple cell types and imaging modalities, demonstrating the method’s scalability and potential for broader applications in medical imaging, cellular biology, and diagnostics.

1 Introduction

Accurate and scalable semantic segmentation of cells in medical imaging is a key challenge with far-reaching implications for diagnostics, research, and personalized medicine. In recent years, deep learning-based methods have gained increasing traction in this fast-moving field. By improving the real-time identification of malignant cells, clinicians can benefit from the objective insights of a computational system, providing a clearer lens to observe and evaluate potential discrepancies or nuances that may be missed in manual assessments. In addition, these technologies could help improve treatment strategies by differentiating resistant cells from non-resistant ones and discerning intricate stages of cancer, such as the blast stage in leukemia. Computational tools appear particularly relevant in cases such as the identification of leukemic cells within heterogeneous populations. In the field of cell segmentation, a diverse landscape of research has emerged, ranging from the segmentation of cell instances [1, 2] to the semantic segmentation of cell classes [5, 6]. While traditional supervised methods have clear advantages, they face inherent challenges, one of which is the need for manual annotation. Manual processes remain time-intensive and prone to errors, even with advanced annotation tools. For instance, the annotation of peripheral blood mononuclear cells (PBMCs) isolated from healthy donors poses its own unique difficulties. Their inherent morphological diversity and close resemblance to other cell types make manual annotation of PBMCs particularly labor-intensive and error-prone or even require fluorescent immunophenotyping markers to label the different groups within PBMCs, underscoring the need for more annotation-independent computational tools. In contrast, unsupervised learning approaches perform well on more straightforward tasks such as foreground segmentation [3, 4]. Yet, when faced with more complex challenges, they often lag behind

*Corresponding author: naouarm@cs.uni-freiburg.de

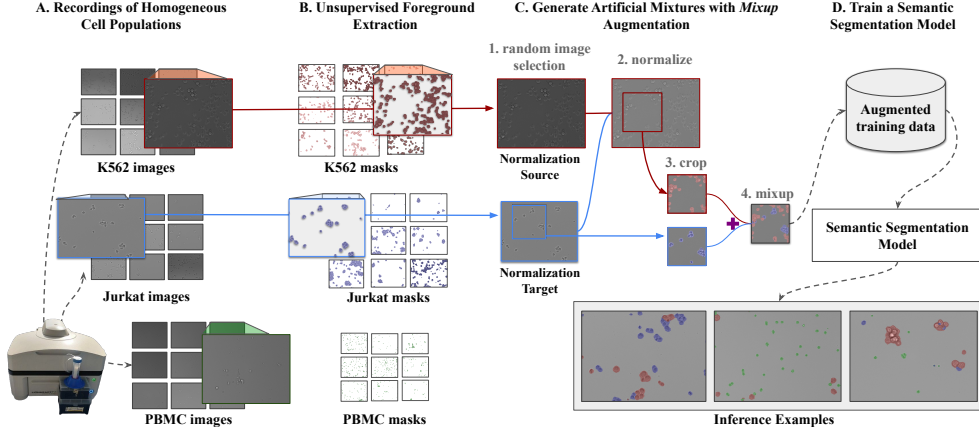


Figure 1: CellMixer Pipeline: (A) Homogeneous Cell Populations are recorded separately with the Lionheart microscope. (B) Foreground annotations are extracted using an unsupervised gradient-based approach and the image label is assigned to each cell. (C) Artificial mixtures are generated using mixup augmentation. (D) A semantic segmentation model is trained from the artificial mixtures.

the results achieved by supervised methods. This highlights the delicate balance of reducing the level of supervision while striving to maintain accuracy. In this landscape, weakly-supervised learning emerges as a compelling middle ground, aiming to balance the benefits of both approaches.

In this work, we introduce CellMixer, a novel augmentation-based strategy aiming to suppress the need for labor-intensive manual annotations. Our weakly-supervised semantic cell segmentation method uses unannotated labeled brightfield images of homogeneous cell populations captured on a Lionheart automated microscope at 20x magnification and comprises four stages (cf. Figure 1). First, we record single-class populations individually. Second, we employ an unsupervised foreground segmentation method to extract single-class clumps of cells. Third, we randomly select pairs of images and normalize their brightness and saturation. Fourth, we employ mixup augmentation [8] to generate artificially annotated mixed populations. This generated dataset of artificial mixtures is then used to train a supervised segmentation model. In our experiments, we applied this approach to simulate realistic clinical conditions by generating artificial mixtures of two different leukemic cell lines, Jurkat and K562, with PBMCs and validated our model on real mixtures of these cells.

2 CellMixer

Unsupervised Foreground Extraction After recording homogeneous populations, we first extract cells from their respective background as a first step towards artificially mixed populations. At its core, our unsupervised foreground segmentation method relies on the inherent contrasts and structures present in such images to distinguish regions of interest from the surrounding environment. Each image I is processed to accentuate its salient structures via the Sobel operators S_x and S_y , which effectively capture the edges, emphasizing transitions in intensity, which often correspond to cell areas in microscopy images. The gradient magnitude of the pixels in each image is then calculated as $G = \sqrt{S_x^2 + S_y^2}$. Smoothing, applied before and after the Sobel operation, provides attenuation of high-frequency noise. This helps to better highlight true cell boundaries. Subsequent refinement by morphological erosion, defined as: $(G \ominus B)(x, y) = \min_{(i, j) \in B} G(x - i, y - j)$, where B is a structuring element for the local neighborhood, helps break small intercellular connections and suppress unimportant structures, ensuring that larger, cohesive structures (cells or cell clusters) are preserved and emphasized. By (adaptively) thresholding the processed gradient magnitudes, a clear segmentation between the cells and the background is achieved. Next, the given image label is assigned to each of its foreground pixels.

Artificial Mixtures Within the training process, two image crops I_1 and I_2 , along with their respective ground truth maps M_1 and M_2 , are randomly selected from the dataset. These are subsequently normalized based on the mean and standard deviation of their background pixels. This

Table 1: Comparison between the segmentation performance of CellMixer with the baseline on homogeneous cell cultures (UnMixed), artificially generated cell mixtures (Artificial Mix), real jurkat+K562 cell mixtures, and a selection of PBMC+jurkat and PBMC+K562 cell mixtures (Real PJ+PK). The mean accuracy (mAcc) and mean Intersection over Union (mIoU) are reported.

Model	Class	Unmixed		Artificial Mix		Real JK Mix		Real PJ+PK Mix	
		mAcc	mIoU	mAcc	mIoU	mAcc	mIoU	mAcc	mIoU
Baseline	Backgr.	99.11	98.74	99.32	96.60	-	-	-	-
	Jurkat	93.98	87.83	72.79	64.94	62.04	52.18	63.29	46.09
	K562	97.91	92.71	88.20	80.44	71.92	49.99	34.99	34.99
	PBMC	96.17	78.62	56.19	39.43	-	-	-	-
CellMixer	Backgr.	98.72	98.42	98.12	97.19	-	-	-	-
	Jurkat	93.09	82.33	90.41	83.07	76.57	72.65	95.76	66.26
	K562	96.57	89.63	96.68	89.87	90.86	71.99	63.70	63.70
	PBMC	95.0	69.15	91.34	72.28	-	-	-	-

step is crucial to ensure that the brightness and saturation levels of the images align properly before their combination. Note that the mean and standard deviation of all pixels of an image depend on its content, such as its foreground portion. Consequently, normalizing based on the background pixels often provides a more reliable reference for achieving the desired brightness and saturation in the resulting image. Finally, the cell mixing operation combines both images with $\tilde{I} = \lambda I_1 + (1 - \lambda) I_2$, where we empirically set $\lambda = 0.5$. The same operation is then applied to their respective ground truth maps using $\tilde{M} = M_2 + (1 - \text{sign}(M_2)) \cdot M_1$, conditionally overwriting M_1 with M_2 .

Model Training The resulting composite images serve as a robust training set for a semantic segmentation model. This methodology significantly reduces the necessity for manual annotation, thereby expediting the training process and enhancing scalability.

3 Results and Discussion

In our experiments, we compare a segmentation model trained on images from CellMixer (CellMixer) to the baseline which was trained on the original homogeneous cell cultures and their generated ground truth maps (Baseline). Both models are evaluated on four different datasets: the first consisting of a set of images of homogeneous cell cultures, the second of artificially generated heterogeneous cell cultures using CellMixer, and two sets of real heterogeneous cell cultures partially annotated by an expert. More details about the datasets and the experimental setup can be found in Appendix A.1. The results reported in Table 1 show that our method clearly outperforms the baseline on both artificial and real cell mixtures. In particular, the quantitative scores suggest that the baseline achieves a decent performance on unmixed cells, but struggles to segment cell mixtures. Based on the observations from our qualitative analysis (cf. Appendix A.2), it seems apparent that this effect is due to the model’s tendency to assign the same label to nearby foreground pixels. This bias, caused by the fact that the training set of the baseline contains only homogeneous cell mixtures, becomes problematic as soon as the network encounters heterogeneous cell cultures. While CellMixer significantly reduces this bias, the network still tends to assign the same label to cells in the same neighborhood in some rare cases. In addition, the qualitative analysis shows that the most challenging cases for CellMixer occur with very dense cell clusters. However, these are extremely difficult to analyze even for experts due to the limited visibility of occluded cells in the 2D projection.

4 Conclusion

We presented CellMixer, a novel augmentation-based weakly supervised semantic cell segmentation approach. By suppressing the need for annotations, CellMixer greatly reduces the data generation effort by the experts and the number of mislabeled cells, as it is way easier to label homogeneous cell cultures than to annotate every single cell of a heterogeneous culture. To better cover overlapping cells, moving to multi-label segmentation and the generation of more realistic clumps of cells are promising avenues for future work.

Acknowledgments

This project was funded by the Mertelsmann Foundation. This work is part of BrainLinks-BrainTools which is funded by the Federal Ministry of Economics, Science and Arts of Baden-Württemberg within the sustainability program for projects of the excellence initiative II.

References

- [1] S.B. Asha, G. Gopakumar, and Gorthi R.K. Sai Subrahmanyam. Saliency and ballness driven deep learning framework for cell segmentation in bright field microscopic images. *Engineering Applications of Artificial Intelligence*, 118:105704, 2023. ISSN 0952-1976. doi: <https://doi.org/10.1016/j.engappai.2022.105704>. URL <https://www.sciencedirect.com/science/article/pii/S0952197622006947>.
- [2] Thorsten Falk, Dominic Mai, Robert Bensch, Özgün Çiçek, Ahmed Abdulkadir, Yassine Marakchi, Anton Böhm, Jan Deubner, Zoe Jäckel, Katharina Seiwald, Alexander Dovzhenko, Olaf Tieltz, Cristina Dal Bosco, Sean Walsh, Deniz Saltukoglu, Tuan Leng Tay, Marco Prinz, Klaus Palme, Matias Simons, Ilka Diester, Thomas Brox, and Olaf Ronneberger. U-net: deep learning for cell counting, detection, and morphometry. *Nature Methods*, 16(1):67–70, Jan 2019. ISSN 1548-7105. doi: 10.1038/s41592-018-0261-2. URL <https://doi.org/10.1038/s41592-018-0261-2>.
- [3] Liang Han and Zhaozheng Yin. Unsupervised network learning for cell segmentation. In Marleen de Bruijne, Philippe C. Cattin, Stéphane Cotin, Nicolas Padoy, Stefanie Speidel, Yefeng Zheng, and Caroline Essert, editors, *Medical Image Computing and Computer Assisted Intervention – MICCAI 2021*, pages 282–292, Cham, 2021. Springer International Publishing. ISBN 978-3-030-87193-2.
- [4] Carola Krug and Karl Rohr. Unsupervised cell segmentation in fluorescence microscopy images via self-supervised learning. In Mounîm El Yacoubi, Eric Granger, Pong Chi Yuen, Umapada Pal, and Nicole Vincent, editors, *Pattern Recognition and Artificial Intelligence*, pages 236–247, Cham, 2022. Springer International Publishing. ISBN 978-3-031-09037-0.
- [5] Sajith Kecheril Sadanandan, Petter Ranefall, Sylvie Le Guyader, and Carolina Wählby. Automated training of deep convolutional neural networks for cell segmentation. *Scientific Reports*, 7(1):7860, Aug 2017. ISSN 2045-2322. doi: 10.1038/s41598-017-07599-6. URL <https://doi.org/10.1038/s41598-017-07599-6>.
- [6] Saba Saleem, Javeria Amin, Muhammad Sharif, Muhammad Almas Anjum, Muhammad Iqbal, and Shui-Hua Wang. A deep network designed for segmentation and classification of leukemia using fusion of the transfer learning models. *Complex & Intelligent Systems*, 8(4):3105–3120, Aug 2022. ISSN 2198-6053. doi: 10.1007/s40747-021-00473-z. URL <https://doi.org/10.1007/s40747-021-00473-z>.
- [7] Robin Strudel, Ricardo Garcia Pinel, Ivan Laptev, and Cordelia Schmid. Segmenter: Transformer for semantic segmentation. In *ICCV*, pages 7242–7252. IEEE, 2021.
- [8] Hongyi Zhang, Moustapha Cissé, Yann N. Dauphin, and David Lopez-Paz. mixup: Beyond empirical risk minimization. In *ICLR (Poster)*. OpenReview.net, 2018.

A Appendix

A.1 Experimental Setting

A.1.1 Dataset

The dataset consists of labeled brightfield images of homogeneous cell populations captured on a Lionheart automated microscope at 20x magnification resulting in grayscale images with a resolution of 1224×904 pixels. The dataset is highly imbalanced; 2405 of the images are labeled as *Jurkat cells*, 1603 as *K562 cells*, and 588 as *PBMC cells*. The entire dataset is split by withholding 10% of randomly selected images from each cell culture for validation and using the remaining images for training.

For Testing, a dataset consisting of 152 partially annotated images from heterogeneous cell mixtures is used for the validation of our method in a real setting. Note that an exhaustive accurate annotation of a heterogeneous cell culture is challenging even for an expert.

A.1.2 Training Pipeline

We train a deep segmentation model composed of a dinov2 encoder and a Segmenter decoder [7]. The model is trained for 20k Iterations with a batch size of 16 and a crop size of 518.

During training, we apply random flipping, random blurring, random Gaussian noise as well as a random modification of the brightness and contrast of the input image as data augmentation and train our model using the SGD optimizer and the Tversky loss to address the issue of data imbalance. We train our model using a learning rate of 0.001 and without weight decay=0.0.

The inference of the model is performed using a sliding window of size corresponding to the model input size (518).

A.2 Qualitative Examples

Qualitative examples are shown in Figure 2. The baseline’s tendency to assign the same label to all foreground pixels in its field of view can be seen in each example. Moreover, we observe that this bias is considerably reduced by Cellmixer, but not completely suppressed (see (7)). Two examples of the most challenging samples containing very dense cell clusters are presented in (4) and (6)

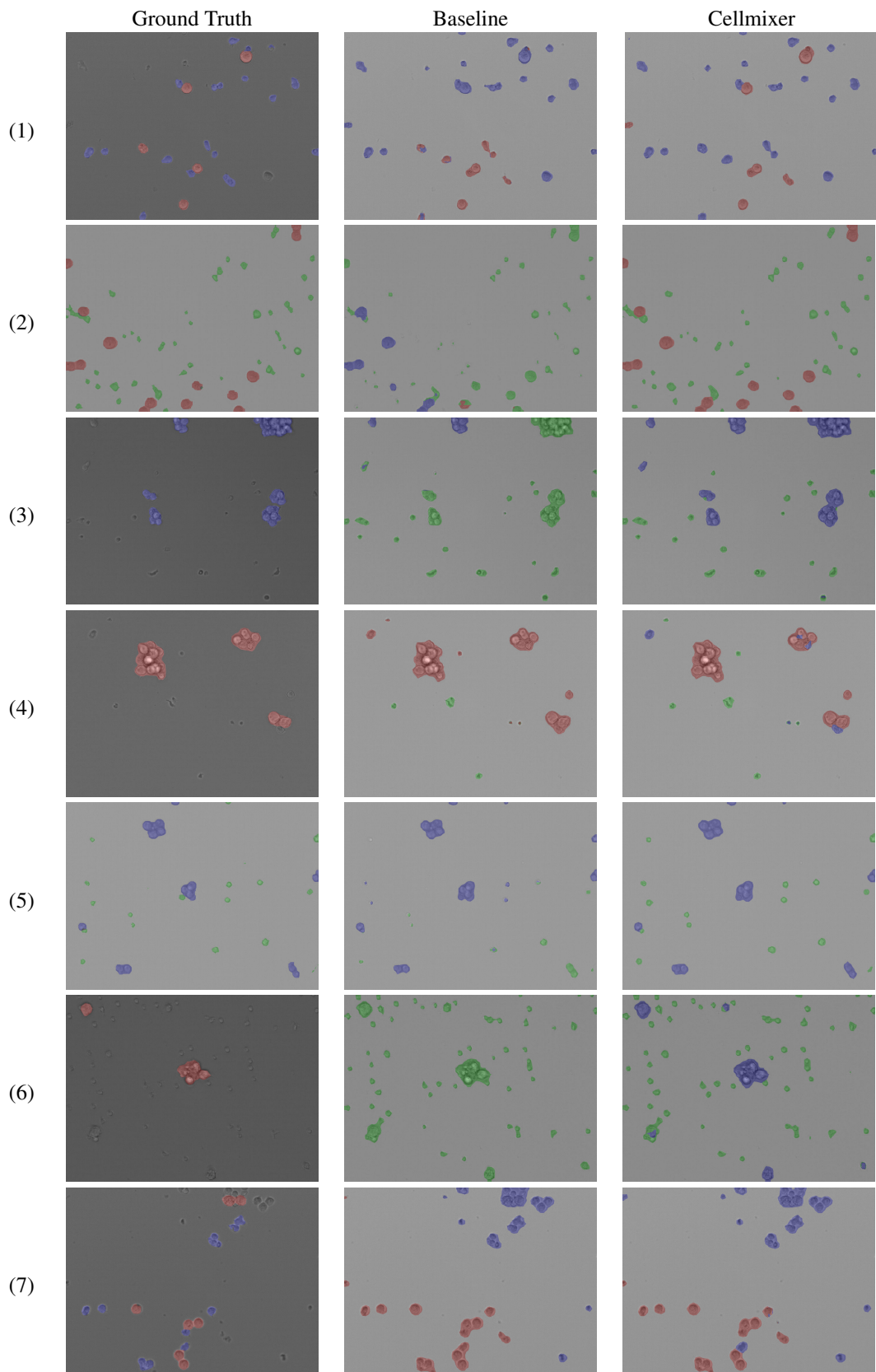


Figure 2: Qualitative examples. Jurkats in blue, K562s in red and PBMCs in green.